Supporting Information

Potentiodynamic Polarization Assisted Phosphorous-containing Amorphous Trimetal Hydroxide Nanofiber for Highly Efficient Hybrid Supercapacitors

Nilesh R. Chodankar[a], G. Seeta Rama Raju[a], Bumjun Park[b], Pragati A. Shinde[c], Seong Chan Jun[c], Deepak P. Dubal[d], Yun Suk Huh[b]*, Young-Kyu Han[a]**

[a]*Department of Energy & Materials Engineering, Dongguk University, Seoul, 100-715, Republic of Korea*

[b]*WCSL of Integrated Human Airway-on-a-Chip, Department of Biological Engineering, Inha University, 100, Inha-ro, Incheon, 22212, Republic of Korea*

[c]*Nano-Electro Mechanical Device Laboratory, School of Mechanical Engineering, Yonsei University, Seoul, 120-749, South Korea*

[d]*School of Chemistry, Physics and Mechanical Engineering, Queensland University of Technology (QUT), 2 George Street, Brisbane, QLD, 4001, Australia*

Corresponding author-

Dr. Deepak P. Dubal – dubaldeepak2@gmail.com

Prof. Yun Suk Huh - yunsuk.huh@inha.ac.kr

Prof. Young-Kyu Han - ykenergy@dongguk.edu

Supporting Information 1

The comparative electrochemical performance for the hybrid supercapacitors reported in the literature.

Positive Electrode	Negative Electrode	Electrolyte	Voltage window (V)	Specific capacitance	Max. Energy density	Max. Power density	Cycling stability (%)	Ref.
MOF-derived Ni/NiO	CNTs-COOH	KOH/PVA	1.8	136.4 F/g @ 2 mA/cm^2	61.3 Wh/kg	9.064 kW/kg	92.8 over 10,000 cycles	[1]
$Co_{2.18}Ni_{0.82}Si_2O_5(OH)_4$	Graphene	KOH/PVA	1.75	194.3 mF/cm^2 @ 0.50 mA/cm^2	0.496 mWh/cm^3	38.8 mW/cm^3	96.3 over 10,000 cycles	[2]
$Co(OH)_2$@Carbonized wood (CW)	Carbonized wood (CW)	KOH/PVA	1.5	14.19 F/cm^3 @ 1 mA/cm^2	0.69 mWh/cm^2 (10.87 Wh/kg)	15.447 W/cm^2 (236.8 W/kg)	85 over 10,000 cycles	[3]
Ni-Co LDH	AC	KOH/PVA	1.6	265 F/g at 1 A/g	94.5	15.6 kW/kg	80.5 over	[4]

					Wh/kg		1000 cycles	
$Ni(OH)_2$/NGP	Mn_3O_4/NGP	NaOH/PVA	1.3	1.96 F/cm^3 @ 50 mV/s	0.35 mWh/cm^3	32.5 mW/cm^3	83 over 12,000 cycles	[5]
$Ni_{0.85}Se$	AC	KOH/PVA	1.6	81 F/g @ 1 A/g	29 Wh/kg	5.512 kW/kg	81.25 over 5,000 cycles	[6]
$Ni_{20}[(OH)_{12}(H_2O)_6][(HP_4)_8(PO_4)_4].12H_2O$	Graphene	KOH/PVA	1.47	0.446 mWh/cm^3 @ 0.5 mA/cm^2	0.446 mWh/ cm^3	44.1 mW/cm^3	97.4 over 5,000 cycles	[7]
NiMn-LDH/CNT	RGO/CNT	KOH/ Nafion	1.7	221 F/g @ of 1 A/g	88.3 Wh/kg	17.2 kW/kg	94 over 1,000 cycles	[8]
$NaCoPO_4$-Co_3O_4	Graphene	KOH/PVA	1.0	28.6 mF/cm^2 @	0.39	50	94.5 over	[9]

				0.1 mA/cm^2	mWh/cm^3	mW/cm^3	5,000 cycles	
$NiCo_2O_4$@PPy	AC	KOH/PVA	1.6	165.4 @ 1 mA/cm^2	58.8 Wh/kg	10.2 kW/kg	89.2 over 5,000 cycles	[10]
Co_3O_4@C@Ni_3S_2	AC	KOH/PVA	1.8	-	1.52 mWh/cm^3	60 W/cm^3	91.43 over 10,000 cycles	[11]
$CoNi_2S_4$/Ni	CNTs+GR/Ni	KOH/PVA	1.8	23.5 F/g (102 mF/cm^3 @ 12 mA/cm^3	10.6 Wh/kg	3.732 kW/kg	77.3 over 1800 cycles	[12]
$Ni_{11}(HPO_3)_8(OH)_6$	Graphene	KOH/PVA	1.4	1.64 F/cm^3@ 0.50 mA/cm^2	0.45 mWh/cm^3	33 mW/cm^3	93.3 over 10,000 cycles	[13]
CoO@NiO/AC textile	AC-textile /graphene	KOH/PVA	1.6	147.6 F/g @ 10 mA/cm^2	52.26 Wh/kg	9.53 kW/kg	97.5 over 2,000	[14]

							cycles	
Carbon Fiber (CF)-$Ni(OH)_2$	CF−CNT	KOH/PVA	1.3	-	41.1 Wh/kg	3.5 kW/kg	98 over 3,000 cycles	[15]
Carbon cloth@$CoMoO_4$@NiCo LDH	AC	KOH/PVA	1.6	167.3 F/g @ 1 A/g	59.5 Wh/kg	16 kW/kg	89.7 over 5000 cycles	[16]
Ni_3S_2	3D-rGO	KOH/PVA	2.2	105 F/g @ 1 A/g	70.58 Wh/kg	33 kW/kg	90.4 over 5000 cycles	[17]
$K_2Co_3(P_2O_7)_2$-$2H_2O$	Graphene	KOH/PVA	1.07	6 F/cm^3 @ 10 mA/cm^3	0.96 mWh/cm^3	54.5 mW/cm^3	94.4 over 5,000 cycles	[18]
NiO+Co_3O_4	Polypyrrole	KOH/PVA	1.5	14.69 F/cm^3 @ 25 mA/cm^3	3.83 mWh/cm^3	29 mWh/cm^3	91 over 6000 cycles	[19]

$FeCo_2O_4$@ polypyrrole	AC	KOH/PVA	1.6	194 F/g @ 1 A/g	68.8 Wh/kg	15.5 kW/kg	91 over 5000 cycles	[20]
$Ni(OH)_2$ @ sulfonated graphene	AC	KOH/PVA	0.8	80.44 F/g @ 0.05 A/g	7.15 Wh/kg	118 W/kg	75 over 1000 cycles	[21]
$CuCo_2S_4$	MoO_2@ N-doped carbon	KOH/PVA	1.6	184 F/g @ 1 A/g	65.1 Wh/kg	12.8 kW/kg	90.6 over 5000 cycles	[22]
$NiCo_2S_4$@ $CoMoO_4$	AC	KOH/PVA	1.6	187.3 F/g @ 1 A/g	66.6 Wh/kg	16 kW/kg	85.6 over 5000 cycles	[23]
$NiMoO_4$-PANI	AC	KOH/PVA	1.6	93 F/g @ 0.3 A/g	33.07 Wh/kg	5.2 kW/kg	98.6 after 5,000 cycles	[24]
$NiCo_2O_4$/CC	Porous	LiOH/PVA	1.8	71.32 F/g @	60.9	11.36	96.8 over	[25]

	graphene paper (PGP)			5 mA/cm^2	Wh/kg	kW/kg	5,000 cycles	
Co_9S_8	Co_3O_4@RuO_2	KOH/PVA	1.6	4.28 F/cm^3 @ 2.5 mA/cm^2	1.44 mWh/cm^3	0.89 W/cm^3	90.2 over 2,000 cycles	[26]
MOF-derived CoO@S-Co_3O_4	MOF-derived carbon	KOH/PVA	1.5	1.99 F/cm^3 @ 2 mA/cm^2	0.71 mWh/cm^3	207 mW/cm^3	87.9 over 5,000 cycles	[27]
$Co_{11}(HPO_3)_8(OH)_6$-Co_3O_4	Graphene	KOH/PVA	1.38	1.84 F/cm^3 @ 0.5 mA/cm^2	0.48 mWh/cm^3	105 mW/cm^3	98.7 over 2,000 cycles	[28]
$CoMoO_4$/PPy	AC	KOH/PVA	1.7	-	104.7 Wh/kg	971.43 W/kg	95 over 2,000 cycles	[29]
Polypyrrole/Ni(O	AC	KOH/PVA	1.6	224 F/g @	79.6	7.97 kW/kg	60 over	[30]

$H)_2$/sulfonated GO				1 A/g	Wh/kg		5,000 cycles	
Ni-Mo-S	Ni-Fe-S	KOH/PVA	1.6	103 mAh/g @ 2 mA/cm^2	82.13 Wh/kg	13.103 kW/kg	95.86 over 10,000 cycles	[31]
$CoMoO_4$@$Co_{1.5}Ni_{1.5}S_4$	AC		1.6	221.3 F/g @ 1.5 A/g	127.86 Wh/kg	6.587 kW/kg	96.3 over 2,000 cycles	[32]
Cobalt carbonate hydroxide/N-doped graphene	N-doped graphene	KOH/PVA	1.9	153.5 mF/cm^2 @ 1.0 mA/cm^2	0.77 Wh/m^2	25.3 W/m^2	93.6 over 2,000 cycles	[33]
NiS/Ni_3S_2	AC	KOH/PVA	1.7	0.34 mAh/cm^2 @ 2 mA/cm^2	0.289 mWh/cm^2	12.825 mW/cm^2	86.7 over 8,000 cycles	[34]
S@Ni-MOF	AC	KOH/PVA	1.6	136.5 F/g @ 1 A/g	56.85 Wh/kg	4.1 kW/kg	86.67 over 20,000	[35]

							cycles	
$Ni_{0.1}Co_{0.8}Mn_{0.1}$	PAN-derived carbon	KOH/PVA	1.6	147 F/g @ 1 A/g	52.47 Wh/kg	8 kW/kg	89.5 over 10,000 cycles	[36]
Mn-Silicate	AC	KOH/PVA	1.2	1.048 F/cm^2 @ 2 mA/cm^2	4.6 mWh/cm^3	80 mW/cm^3	32 over 900 cycles	[37]
Co-Silicate	AC	KOH/PVA	1.5	0.375 F/cm^2 @ 2 mA/cm^2	2.6 mWh/cm^3	98 mW/cm^3	45 over 2,800 cycles	[37]
Ni-Silicate	AC	KOH/PVA	1.6	0.12 F/cm^2 @ 2 mA/cm^2	0.93 mWh/cm^3	102 mW/cm^3	42 over 3,000 cycles	[37]
PPy@NiCo$(OH)_2$	AC	KOH/PVA	1.4	307 F/g @ 1 A/g	-	-	93 over 5,000 cycles	[38]
$CuGa_2O_4$/NF	FeP/NF	KOH/PVA	1.5	202 F/g @	63.15	9 kW/kg	90 over	[39]

				1 A/g	Wh/kg		5,000 cycles	
CoSe	AC	KOH/PVA	1.4	18.1 mF/cm^2 @ 0.5 mA/cm^2	0.17 mWh/cm^3	33.16 mW/cm^3	96.7 over 5,000 cycles	[40]
$NiCo_2O_4$-GO/CF	P-doped GO/CF	KOH/PVA	2.0	73.3 F/cm^3 @ 0.146 A/cm^3 (100 F/g @ 0.21 A/g)	36.77 mWh/cm^3 (50.6 Wh/kg)	1068 mWh/cm^3 (1.5 kW/kg)	97 over 2,000 cycles	[41]
$NiCo_2S_4$	rGO-hydrogel	KOH/PVA	1.5	110.8 F/g @ 2 A/g	22.21 Wh/kg	-	No Loss after 5000 cycles	[42]
$Ni(OH)_2$@$NiCo_2O_4$@CNTF	VN@CNTF	KOH/PVA	1.6	291.9 mF/cm^2 (106.1 F/cm^3) @ 1 mA/cm^2	0.1038 mWh/cm^2	8 mW/cm^2	87.2 over 5000 cycles	[43]

Graphite nanosheet@$CoMoS_4$	AC	KOH/PVA	1.8	95.11 F/g @ 1 A/g	42.85 Wh/kg	4.5 kW/kg	93.2 over 8000 cycles	[44]
NiO@carbon nanofibers/CC	N-Carbon nanofibers /CC	KOH/PVA	1.5	62.4 F/g @ 20 mA/cm^2	19.5 Wh/kg	11.5 kW/kg	-	[45]
$NiCo_2O_4$	N-doped porous carbons	KOH/PVA-PEO	1.6	120 F/g @ 1 A/g	42.7 Wh/kg	8 kW/kg	94 over 10,000 cycles	[46]
MnO_2	$CoSe_2$	LiCl/PVA	1.6	1.77 F/cm^3 @ 1 mA/cm^2	0.588 mWh/cm^3	0.282 W/cm^3	94.8 after 2,000 cycles	[47]
Ti_3C_2/Ni-Co-Al-LDH	AC	KOH/PVA	1.6	128.89 F/g @ 0.5 A/g	45.8 Wh/kg	6.93 kW/kg	97.8 after 10,000 cycles	[48]
NiCoAl-	AC	KOH	1.6	194 F/g @ 1 A/g	71.7	20000 W/kg	98 % after	[49]

LDH/V_4C_3					Wh/kg		10,000 cycles	
$NiCo_2Al$-LDH	MOF derived porous carbón	KOH/PVA	1.5	144 F/g @ 0.5 A/g	44 Wh/kg	6286 W/kg	91.2 % after 15,000 cycles	[50]
Ni-V-LDH	AC	KOH/LiCl	1.6	91 mF/cm^2 @ 0.1 mA/cm^2	0.24 mW h/cm^3	214.4 mW/cm^3	100 % after 15,000 cycles	[51]
MnSi	AC	KOH/PVA	1.2	1048.3 mF/cm^2 @ 2 mA/cm^2	4.6 mWh/cm^3	-	1000 cycles	[52]
$Ni_2P_2O_7$/Ni-Co-hydroxide	AC	KOH/PVA	1.6	2.99 F/cm^3 @ 2 mA/cm^2	78 Wh/kg	2814 W/kg	91.83 % after 10,000	[53]

							cycles	
$MnO_2@Ni_2P_2O_7$	AC	KOH/PVA	1.6	82 mA h/g @ 1 A/g	66 Wh/kg	1920 W/kg	91.83 % after 10,000 cycles	[54]

Supporting Information 2

Experimental details: All required chemicals were purchased from the Sigma-Aldrich including the Cobalt nitrate ($Co(NO_3)_2{\cdot}_6H_2O$), ruthenium(III) chloride hydrate ($RuCl_3{\cdot}xH_2O$), potassium phosphate monobasic, KOH and hydrochloric acid (HCl). All the required solutions was prepared in the deionised (DI) water. Prior to the deposition of material, the nickel foam was cleaned with the 2 m HCl, DI water, and acetone and then dried at 25 °C for 6 h. To prepare the nickel ruthenium cobalt hydroxide (NRC-OH) thin film over the Ni foam, the potentiodynamic polarization was used for different deposition cycles. The growth solution was prepared by dissolving the 0.01 M of $Co(NO_3)_2{\cdot}6H_2O$ and $RuCl_3{\cdot}xH_2O$ in 40 ml of DI water with continuous stirring for 30 min. Note that the Ni foam itself acts as a source of the Ni. The deposition was carried out in standard three electrode system in which the Ni foam (1 x 2 cm), saturated calomel electrode (SCE), platinum was used as a working, reference and counter electrode within potential window of -1.0 to 0 V/SCE. The deposition was carried out for the 50, 100 and 150 cycles to optimise the proper nanostructure for the SCs application. Among that, NRC-OH100 sample shows the good electrochemical features and therefore it is used for the P-doping. To prepare the P@NRC-OH electrode, the same precursor solution was used and which is diluted with the 0.1 M of potassium phosphate monobasic (5 ml). The deposition was carried out for the 100 cycles. The calculated mass loading of the deposited material over the Ni foam current collector varies from the 1.1 to 1.46 mg/cm^2. The mass loading of the electroactive material is calculated by taking the mass difference of the current collector before and after deposition of the electroactive material.

Electrochemical Measurement: To decide the best electrode for the SC application, initially three electrode electrochemical measurements was performed in the 2 M KOH electrolyte. The CV, GCD and EIS measurements was performed with the Zive sp1 electrochemical workstation. The EIS measurements was performed in the frequency range of 100 kHZ to 10 mHZ at constant bias potential of 10 mV. The CV and GCD measurements was performed at various scanning rate and current densities within potential window of the 0-0.6 V/SCE and 0-0.4 V/SCE, respectively. The two electrode electrochemical measurements was carried out by assembling the hybrid solid state supercapacitor (HSSC) in which P@NRC-OH electrode was used as positive electrode and activated carbon (AC) electrode as a negative electrode in PVA-KOH gel electrolyte. The AC electrode was prepared by using the traditional slurry coating method. To prepare the AC electrode the 80 wt% commercial activated carbon, 10 wt% acetylene black, 5 wt% PVDF, and a small amount of ethanol was prepared by milling to produce a homogeneous paste. The prepared paste was loaded on the nickel foam and heated at 150 °C for 30 min to obtain a well-adherent film of activated carbon. The PVA–KOH gel electrolyte was prepared by mixing 2 M KOH and 2 g of PVA in 20 ml of DI water at 70 °C for 20 min while stirring. The formed transparent gel-like solution was used to assemble the hybrid solid-state supercapacitor.

Calculations

Prior to assemble the HSSC, the mass balancing was carried out from positive to negative electrode by using the following relation;

$$\frac{m_+}{m_-} = \frac{C_- V_-}{C_+ V_+} \qquad \text{(S1)}$$

Where, *m*, *C* and *V* are the mass (m/cm^2), capacitance and the potential window for the positive and negative electrode. The calculated mass ration from the positive to negative electrode is 1:4.88. Furthermore, the specific capacity, areal capacitance, specific energy and specific power were calculated by considering the following equations;

Specific capacity from the CV

$$Specific\ capacity\ (Ah/g) = \frac{\int i(V)dV\ (A.V)}{m\ (g) \times \vartheta\ (V/s) \times 3600} \qquad \text{(S2)}$$

where, the integration of current over voltage window will give the total voltammetric charge in A.V (ampere*volts). ν is scan rate and *m* is the mass loading.

Specific capacity from the GCD

$$Specific\ capacity\ (mA\ h/g) = \frac{i.\Delta t}{m.\ 3.6} \qquad \text{(S3)}$$

where, I is the applied current, Δt is the discharging time, m is the mass loading.

Areal capacitance

$$areal\ capacitance = \frac{i\int vdt}{AV} \tag{S4}$$

where, ΔV is the voltage window.

Specific energy (Wh/kg) and specific power (W/kg)

$$Specific\ energy = \frac{C.\Delta V^2}{2\times\ 3600} \tag{S5}$$

$$Specific\ power = \frac{3600\ \times specific\ energy}{\Delta t} \tag{S6}$$

Energy efficiency

$$energy\ effeciency\ (\%) = \frac{discharge\ specific\ energy\ \times 100}{charge\ specific\ energy} \tag{S7}$$

Supporting Information 3

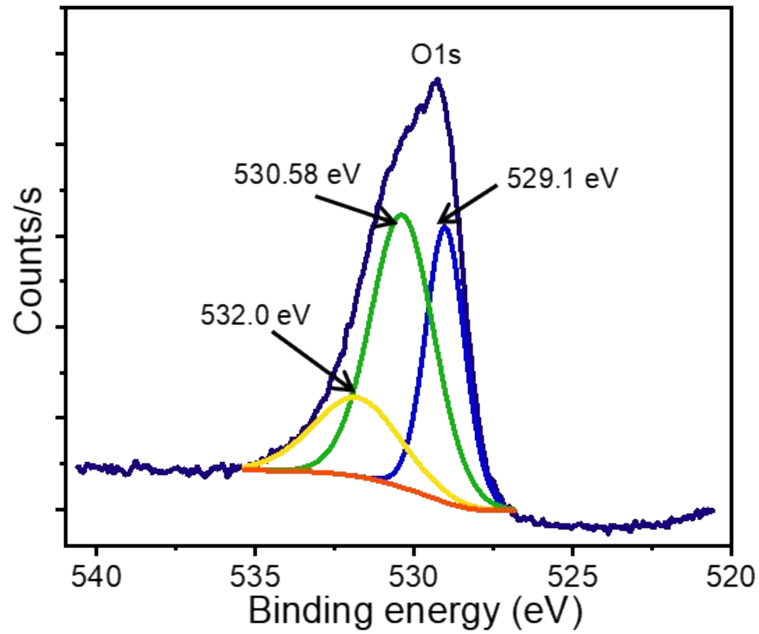

Fig. S1 core-level O1s XPS spectra for the P@NRC-OH sample

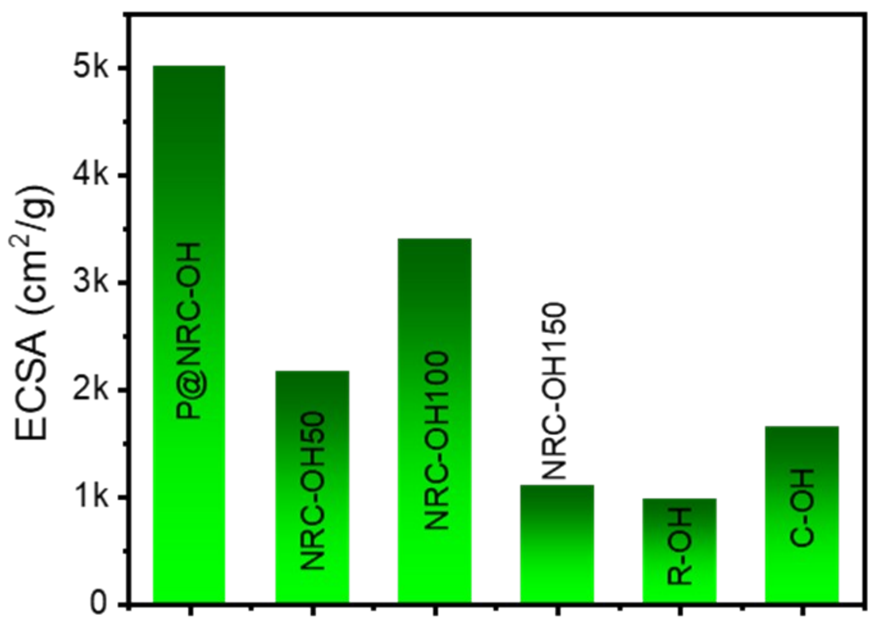

Fig. S2 the electrochemical surface area (ECSA) for all samples.

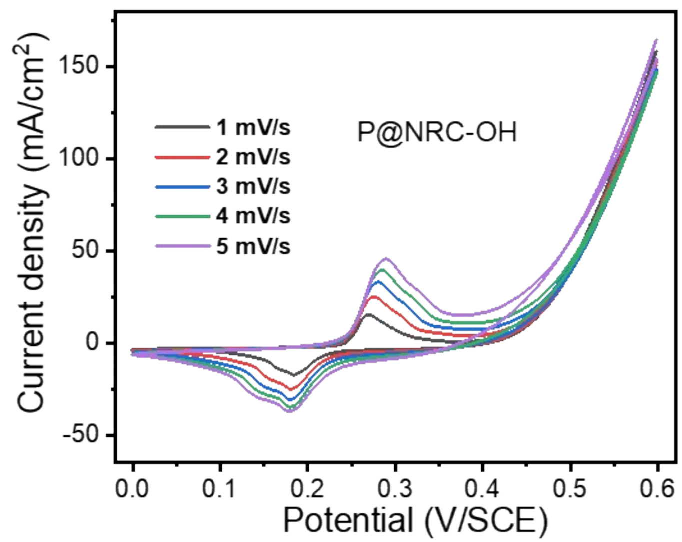

Fig. S3 the CV curves for the P@NRC-OH electrode at scanning rate of 1, 2, 3, 4, 5 mV/s.

References

[1]	Y. Jiao, W. Hong, P. Li, L. Wang, G. Chen, Appl. Cat. B: Environ. 2019, 244, 732-739
[2]	J. Zhao, M. Zheng, Z. Run, J. Xia, M. Sun, H. Pang, J. Power Sources, 2015, 285, 385.
[3]	Y. Wang, X. Lin, T. Liu, H. Chen, S. Chen, Z. Jiang, J. Liu, J. Huang, M. Liu, *Adv. Funct. Mater.* 2018, 28, 1806207
[4]	W. Zou, W. Guo, X. Liu, Y. Luo, Q. Ye, X. Xu, F. Wang, *Chem. Eur. J.* 2018, 24, 19309-19316
[5]	J. X. Feng, S. H. Ye, X. F. Lu, Y. X. Tong, G. R. Li, *ACS Appl. Mater. Interfaces*, 2015, 7, 11444.
[6]	A. Ye, Y. Sui, J. Qi, F. Wei, Y. He, Q. Meng, Y. Ren, Z. Sun, *J. Electronic Mater.* 2018, 47, 7002-7010
[7]	J. Zhao, S. Wang, Z. Run, G. Zhang, W. Du, H. Pang, Part. Part. Syst. Charact., 2015, 32, 880.
[8]	J. Zhao, J. Chen, S. Xu, M. Shao, Q. Zhang, F. Wei, J. Ma, M. Wei, D. G. Evans, X. Duan, Adv. Funct. Mater., 2014, 24, 2938.
[9]	C. Wei, C. Cheng, B. Zhou, X. Yuan, T. Cui, S. Wang, M. Zheng, H. Pang, Part. Part. Syst. Charact. 2015, 32, 831.
[10]	D. Kong, W. Ren, C. Cheng, Y. Wang, Z. Huang, H. Y. Yang, ACS Appl. Mater. Interfaces, 2015, 7, 21334.
[11]	D. Kong, C. Cheng, Y. Wang, J. I. Wong, Y. Yang, H. Y. Yang, J. Mater. Chem. A, 2015, 3, 16150.
[12]	J. Song, Y. Chen, K. Cao, Y. Lu, J. H. Xin, X. Tao, *ACS Appl. Mater. Interfaces* 2018, 10, 39839
[13]	Y. Gao, J. Zhao, Z. Run, G. Zhang, H. Pang, *Dalton Trans.*, 2014, 43, 17000.
[14]	Z. Gao, N. Song, X. Li, *J. Mater. Chem. A*, 2015, 3, 14833.

[15]	D. Ghosh, M. Mandal, C. K. Das, *Langmuir*, 2015, 31, 7835.
[16]	Y. Zhao, X. He, R. Chen, Q. Liu, J. Liu, J. Yu, J. Li, H. Zhang, H. Dong, M. Zhang, J. Wang, Chem. Eng. J. 2018, 352, 29-38
[17]	C. Zhang, S. Wang, S. Tang, S. Wang, Y. Li, Y. Du, Appl. Surf. Sci. 2018, 458, 656-664
[18]	H. Pang, Y. Zhang, W. Y. Laib, Z. Huc, W. Huang, Nano Energy, 2015, 15, 303.
[19]	J. Wen, B. Xu, J. Zhou, Y. Chen, J. Power Sources 2018, 402, 91-98
[20]	X. He, Y. Zhao, R. Chen, H. Zhang, J. Liu, Q. Liu, D. Song, R. Li, J. Wang, *ACS Sustainable Chem. Eng.* 2018, 6, 14945−14954
[21]	H. Gao, C. Hao, Y. Qi, J. Li, X. Wang, S. Zhou, C. Huang, *J. Alloys Comp.* 2018, 767, 1048-1056
[22]	S. Liu, Y. Yin, K. S. Hui, K. N. Hui, S. C. Lee, S. C. Jun, *Adv. Sci.* 2018, 5, 1800733
[23]	Y. Zhao, X. He, R. Chen, Q. Liu, J. Liu, D. Song, H. Zhang, H. Dong, R. Li, M. Zhang, J. Wang, Appl. Surf. Sci. 2018, 453, 73–82
[24]	H. Gao, F. Wu, X. Wang, C. Hao, C. Ge, Int. J. Hydrogen Energy, 2018, 43, 18349-18362
[25]	Z. Gao, W. Yang, J. Wang, N. Song, X. Li, Nano Energy, 2015, 13, 306.
[26]	J. Xu, Q. Wang, X. Wang, Q. Xiang, B. Liang, D. Chen, G. Shen, ACS nano, 2013, 7, 5453.
[27]	S. Dai, Y. Yuan, J. Yu, J. Tang, J. Zhou, W. Tang, *Nanoscale*, 2018, 10, 15454–15461
[28]	Y. Zhang, M. Zheng, M. Qu, M. Sun, H. Pang, J. Alloys Compd., 2015, 651, 214.

[29]	Y. Chen, B. Liu, Q. Liu, J. Wang, Z. Li, X. Jing, L. Liu, Nanoscale, 2015, 7, 15159.
[30]	J. Li, C. Hao, S. Zhou, C. Huang, X. Wang, *Electrochim. Acta* 2018, 283, 467-477
[31]	J. Balamurugan, C. Li, V. Aravindan, N. H. Kim, J. H. Lee, *Adv. Funct. Mater.* 2018, 28, 1803287
[32]	C. Wang, Z. Guan, Y. Shen, S. Yu, X. Z. Fu, R. Sun, C. P. Wong, *Chem. Eng. J.* 2018, 346, 193-202
[33]	H. Xie, S. Tang, J. Zhu, S. Vongehr, X. Meng, *J. Mater. Chem. A*, 2015, 3, 18505.
[34]	F. Chen, H. Wang, S. Ji, V. Linkov, R. Wang, *Mater. Today Energy* 2019, 11, 211-217
[35]	L. Yue, H. Guo, X. Wang, T. Sun, H. Liu, Q. Li, M. Xu, Y. Yang, W. Yang, *J. Colloid Interface Sci.* 2019, 539, 370-378
[36]	Y. Liu, N. Liu, L. Yu, X. Jiang, X. Yan, *Chem. Eng. J.* 2019, 362, 600–608
[37]	Q. Wang, Y. Zhang, H. Jiang, X. Li, Y. Cheng, C. Meng, *Chem. Eng. J.* 2019, 362, 818-829
[38]	X. Wu, M. Lian, Q. Wang, *Electrochim. Acta* 2019, 295, 655-661
[39]	A. M. Zardkhoshoui, S. S. H. Davarani, *J. Alloys Comp.* 2019, 773, 527-536
[40]	X. Zhang, J. Gong, K. Zhang, W. Zhu, J. C. Li, Q. Ding, *J. Alloys Comp.* 2019, 772, 25-32
[41]	C. Zhou, T. Gao, Y. Wang, Q. Liu, Z. Huang, X. Liu, M. Qing, D. Xiao, *Small* 2019, 15, 1803469
[42]	F. Lu, M. Zhou, K. Su, T. Ye, Y. Yang, T. D. Lam, Y. Bando, X. Wang, *ACS Appl. Mater. Interfaces* 2019, 11, 2082-2092
[43]	X. Wang, J. Sun, J. Zhao, Z. Zhou, Q. Zhang, C. Wong, Y. Yao, *J. Phys. Chem. C* 2019, 123, 985-993
[44]	M. Wei, C. Wang, Y. Yao, S. Yu, W. H. Liao, J. Rene, R. Sun, C. P. Wong, Chem. Eng. J. 2019, 355, 891-900

[45]	Y. N. Liu, J. N. Zhang, H. T. Wang, X. H. Kang, S. W. Bian, *Mater. Chem. Front.,* 2019, 3, 25-31
[46]	Y. Liu, X. Wang, X. Jiang, X. Li, L. Yu, *Nanoscale*, 2018, 10, 22848-22860
[47]	N. Yu, M. Q. Zhu, D. Chen, *J. Mater. Chem. A*, 2015, 3, 7910.
[48]	R. Zhao, M. Wang, D. Zhao, H. Li, C. Wang, L. Yin, *ACS Energy Lett.*, 2018, 3, 132-140
[49]	X. Wang, H. Li, H. Li, S. Lin, J. Bai, J. M. Dai, C. H. Liang, X. B. Zhu, Y. P. Sun, S. X. Dou, J. Mater. Chem. A 2019, 7, 2291
[50]	X. Gao, X. Liu, D. Wu, B. Qian, Z. Kou, Z. Pan, Y. Pang, L. Miao, J. Wang, Adv. Funct. Mater. 2019, 1903879
[51]	A. Tyagi, M. Joshi, K. Agarwal, B. Balasubramaniam, R. K. Gupta, Nanoscale Adv., 2019, 1, 2400–2407.
[52]	Q. Wang, Y. Zhang, H. Jiang, X. Li, Y. Cheng, C. Meng, Chemical Engineering Journal 2019, 362, 818–829.
[53]	N. R. Chodankar, D. P. Dubal, Su-Hyeon Ji, Do-Heyoung Kim, Small 2019, 15, 1901145
[54]	N. R. Chodankar, D. P. Dubal, S. J. Patil, G. Raju, S. V. Karekar, Y. S. Huh, Young-Kyu Han, Electrochimica Acta 2019, 319, 435.